A Novel Algorithm for EMG Signal Processing and Muscle Timing Measurement

Simone Pasinetti, Matteo Lancini, Ileana Bodini, and Franco Docchio

***Abstract*— This paper presents a new method for the automated processing of surface electromyography (SEMG) signals, particularly suited for the detection of muscle activation timing. The method has an intermediate level of complexity between simpler (but less performing) and more complex (but in general slower) methods, and is successfully used in the development of biomedical devices for rehabilitation carried out by our group. The method proposed here is based on a statistical approach for threshold computation that is implemented without the need of maximum voluntary contraction or relaxed state, usually required to overcome the difficulty in obtaining the threshold value. The method is compared with 10 popular automated standard methods using different types of simulated signals that approximate the behavior of real SEMG signals. Both the number of activations detected and the onset time measured are analyzed. The algorithm is then applied to real SEMG signals acquired from healthy subjects. The results are finally compared with the literature values. The results show that the proposed algorithm is the best performing method when both the number of activations and the activation timing are considered. In real applications, the algorithm gives the results compatible with the well-agreed literature data.**

***Index Terms*— Activation analysis, electromyography, measurement, muscles, signal processing, timing.**

I. Introduction

SURFACE electromyography (SEMG) is a widely used technique for the evaluation of posture and movement [1]. SEMG analysis frequently requires the estimation of muscle activation timing, as in the case of the functional characterization of the human movement, or of the study of muscle synergies [2]. Muscle timing detection could also be useful in amputated subjects, where the SEMG signal may be used for the control of the prosthesis [3].

Muscle timing detection is defined as the measurement of the muscle onset, i.e., the instant when the muscle goes from a relaxed state to a contracted one, and the muscle offset, i.e., the instant when the muscle returns to the relaxed state, during a single movement cycle. From these two measurements, the duration of activation can also be computed. So far, the most common method to measure the muscle onset is still visual inspection of raw SEMG signals, despite its poor reproducibility [4]. In fact, visual inspection strongly depends on the skill and experience of the examiner and suffers from a high subjectivity between testers and intratesters [5].

To reduce the measurement variability and duration, a considerable amount of research has been focused on computer-based methods for muscle timing detection. These methods range from the simplest ones, which use single or double thresholds to discriminate periods with contracted muscle from periods with relaxed muscle, to more complex ones, which use signal processing techniques, such as wavelet transforms and SEMG signal modeling.

Single- and double-threshold methods usually perform a three-stage signal treatment. This includes: 1) a filtering stage (i.e., low-pass, bandpass, or moving average filtering [6]); 2) a baseline measurement stage (performed measuring the signal amplitude during muscle relaxation or during the subject's maximal voluntary contraction [7], [8]); and 3) a threshold computation stage (computed using the standard deviation of the baseline value). This group of methods needs to set many parameters (filter cutoff frequency, baseline length, etc.). These settings, in term, are based on the signal morphology, and depend on the envisaged application. Furthermore, in some cases, the nature of the algorithm is not adequate to provide both muscle offset and contraction duration, and, for this reason, they are mostly used for signal onset estimation only. Simple methods, such as the ones described above, are frequently used even today in various applications, such as prosthetic hand control [3] and eyeglass prescription [9].

The more sophisticated methods use wavelet transformations to calculate thresholds from the frequency content of a local portion of the SEMG signal [10]. Other methods use modeling techniques to reproduce the shape of the SEMG signal [11]–[13] (in fact, at least theoretically, if two SEMG patterns are similar, the onset/offset detection yields the same results [2]). These methods show a high accuracy and yield more information about the muscle activity. However, some of them are time consuming, require a strong computation, and need to set a large number of parameters; some others, such as [14], differentiate clean signals from their contaminants, but require a conspicuous training period on clean SEMG signals to achieve good results.

Our group is in progress with collaborative developments of biomedical devices. Examples are: 1) an exoskeleton for assisted walk rehabilitation and 2) an orthosis for hand rehabilitation. Both devices need real-time EMG analysis for ideal performance/evaluation. Thus, the effectiveness of the EMG-processing method should be combined with its simplicity and speed of execution. We thus developed, and

Manuscript received March 20, 2015; revised April 28, 2015; accepted April 30, 2015. Date of publication June 3, 2015; date of current version October 7, 2015. The Associate Editor coordinating the review process was Dr. Kurt Barbe.

S. Pasinetti, M. Lancini, and F. Docchio are with the Department of Mechanical and Industrial Engineering, University of Brescia, Brescia 25100, Italy (e-mail: simone.pasinetti@unibs.it).

I. Bodini is with the Department of Information Engineering, University of Brescia, Brescia 25100, Italy.

Digital Object Identifier 10.1109/TIM.2015.2434097

present here, a novel method for muscle timing detection. This method may be considered at the upper level of the category of simple methods, with a performance close to that of more complex methods, but with a much higher simplicity. It uses a single threshold to find muscle activations. Filtering is performed by computing the root-mean-square (rms) value of the SEMG signal. After the filtering stage, a statistical approach is used to find a threshold value for optimal onset detection. The combination of rms-based filtering and statistical approach represents the novelty of our method, with no training required before the muscle activation analysis. The computed threshold is then processed by adding a range of hysteresis, to eliminate the spurious activation detections due to the residual spikes not removed by the filtering stage. Furthermore, the statistical approach is important to simplify the signal treatment by eliminating the baseline computation stage.

This approach needs the setting of only four parameters and a low level of computation. In addition, the calculation of the threshold value does not require preliminary noise level measurements. For these reasons, the proposed method can be used when the measurement of the maximum voluntary contraction is difficult, when the identification of the baseline period is not possible, and/or when the instrumentation used is more susceptible to the environmental electrical noise.

In this paper, we describe the method developed, compare it against the most popular automatic detection methods, and apply it to real SEMG signals obtained from healthy subjects to analyze its behavior in a real application.

II. Description of the Algorithm

The scheme of the signal treatment for muscle timing detection, able to detect both muscle onset and offset, is shown in Fig. 1.

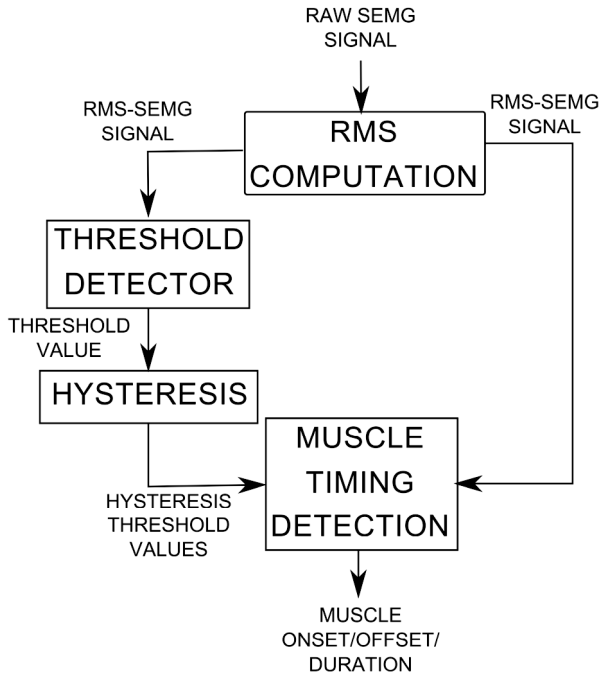

Fig. 1. Scheme of the phases performed in the proposed algorithm for the onset detection.

A. RMS Computation

As a first step, the rms value is extracted from the electromyographic signal. The raw SEMG signal is divided into overlapping rectangular windows of equal amplitude T, each delayed by a time s. The rms–SEMG signal is computed for each ith window using (1). Here, x represents the amplitude of the raw SEMG signal, t is the time, T is the window width, and s is the delay between successive windows

$$\mathrm{RMS}(is) = \sqrt{\frac{1}{T}\int_{is-\frac{T}{2}}^{is+\frac{T}{2}} x^2 dt}. \tag{1}$$

The width of each window represents a tradeoff between the smoothness of the filtered SEMG signal and the alteration of the timing information of the signal. In fact, higher T values mean larger portions of the raw SEMG signal in each window, resulting in a smoothed rms–SEMG signal that avoids false activations (such as activations when the muscle is relaxed). On the other side, lower T values increase the accuracy in the activation detection time [15].

The results of the rms computation are placed in the midpoint of each window, thus the delay parameter s sets the time resolution of rms–SEMG signal. A lower s results not only in a better accuracy in the estimation of the muscle onset, but also in a higher rms–SEMG computation time. The combination of T and s defines window overlapping.

RMS calculation is here appropriate, since it reflects more accurately the behavior of the muscle motor units during muscle contractions [16]. Kamen and Gabriel [17] suggest that there is a quasi-linear relationship between the rms and the magnitude of the SEMG signal. Thus, rms is a good indicator to measure muscle activations. Moreover, in applications when the SEMG signal is used to control actuators [18], [19], the control using the rms–SEMG signal is more efficient than the control using the signal derived from low-pass filtering [20], [21].

B. Threshold Detector

The second stage of signal processing is the main stage of the algorithm and deals with the threshold computation to discriminate between contraction and relaxation. Our algorithm uses a statistical approach to find the right threshold. The amplitude distribution of the whole rms–SEMG signal is evaluated, and the 5th and the 95th percentiles are selected to compute a weighted average as follows:

$$\mathrm{Threshold} = [p_{95} * w + p_5 * (1 - w)] \tag{2}$$

where p_i is the ith percentile of the amplitude distribution of the rms–SEMG signal, and w is the weight used for the computation.

Compared with the standard methods for threshold computation, the 95th percentile could be approximated with the maximum voluntary contraction, while the 5th percentile is used as an approximation of the noise level when muscles are relaxed (similar to a baseline value in standard methods). Using the percentiles instead of the maximum voluntary

contraction and the baseline level greatly reduces the likelihood of misreading the information.

The amplitude distribution of the rms–SEMG signal depends on the type of muscle activation during each movement cycle. In general, the distribution has a bimodal trend, with the two main modes corresponding to the baseline level (the lower one) and the contraction level (the higher one). The cumulative distribution of the rms–SEMG has a behavior characterized by a higher slope at the beginning (due to the signal amplitude when the muscle is relaxed) and at the end (due to the signal amplitude when the contractions occur), and with a lower slope between these two. The threshold for the muscle activations must be placed within the interval of values with lower slope, which represent the values between the two modes in the distribution of the rms–SEMG signal, setting the weight w in (2).

Analyzing the cumulative distribution of the rms–SEMG signal, appropriate values of w are between 0.2 and 0.6. This range strongly depends on the type of muscle activation, because muscles that remain more relaxed during one single cycle of movement move the lower limit toward higher values, while muscles with long contractions move the higher limit toward lower values, thus reducing the range of appropriate weights. A higher noise level [a lower signal-to-noise ratio (SNR)] reduces the feasible range since the modes are closer, whereas a lower noise level increases the range since the modes are more separated.

Within this range, values close to the lower level (0.2) are more sensitive to lower muscle activations, but could lead to errors due to signal noise. In contrast, values close to the higher level (0.6) are more insensitive to signal noise, but could detect a delayed muscle timing. Hence, the weight value generally depends on the type of movement that generates the SEMG signal, and must be analyzed before the signal processing.

C. Hysteresis

The last stage of the algorithm is the computation of the level of hysteresis that is added to the threshold to avoid false onset–offset readings. Two different limits, one higher and one lower than the computed threshold, are used for the detection of the rising and the falling signal crossing edges, respectively, using

$$\begin{aligned} \text{Threshold}_{\text{HIGH}} &= \text{Threshold} * (1 + k) \\ \text{Threshold}_{\text{LOW}} &= \text{Threshold} * (1 - k). \end{aligned} \tag{3}$$

The muscle is considered active when the rms–SEMG signal exceeds the upper limit, and relaxed when it is below the lower limit. Between these two limits, the muscle is considered as in its previous state to get a more robust onset detection.

k is the parameter representing the amplitude of the hysteresis range. It strongly depends on the smoothness level of the rms–SEMG signal, and thus on the parameters used during the rms computation (window length and overlapping). In general, lower window lengths lead to higher k values.

D. Calibration of the Algorithm Parameters

As described above, the algorithm is based on the four parameters s, T, w, and k. The choice of the values of these parameters requires a knowledge of the activation and deactivation times as accurate as possible. Since these two values have a large variability in the literature, the calibration was performed using a set of experimental data, with the aid of an expert in SEMG reading. This approach, typical of many biosignal measurements, is consistent with the definition of a quantity value being a number and a reference to a measurement procedure in the Guide to the Expression of Uncertainty in Measurements (Joint Commitee for Guides in Metrology) [22]. Three healthy subjects were used. All of them were asked to follow a straight path on a plane surface at a comfortable speed. During each walk, the SEMG signals from the *soleus* muscle were acquired. Foot switch sensors were used to split each stride. For each subject, 10 strides were chosen randomly from the walk, resulting in a total number of 30 strides. The activation and deactivation times of each stride were read by the expert in SEMG-gait analysis. All these individual values were found to be consistent with those of [23].

The calibration was performed as follows: initially, parameter s was arbitrarily fixed to 0.01 s to maintain a high resolution for the rms computation phase. Parameters T, w, and k were derived from the 30 activation and deactivation time values using a minimization procedure. First, the three parameters were given arbitrary values: with these initial values our algorithm was used to compute the activation ($t_{\text{ACT,ALG},i}$) and deactivation ($t_{\text{DEACT,ALG},i}$) times of each stride ($i = 1{-}30$). Then, the value ε_i, i.e., the quadratic sum of the difference between the calculated and expert values (the latter being $t_{\text{ACT,EXP},i}$ and $t_{\text{DEACT,EXP},i}$) was computed using (4), as shown at the bottom of this page.

The procedure was repeated by varying T, w, and k within their admissible range, until the minimum value of ε_i was reached.

Repeating the minimization procedure for all 30 strides, and calculating the mean and the standard deviation of all the resulting parameters, the data reported in Table I were obtained.

The mean values for T, w, and k were the result of the calibration procedure.

III. Results

This section is devoted to the evaluation of the performances of the method proposed. First, we compared our method against the common automatic methods present in the literature and mostly used by clinicians. For this purpose, we used the simulated SEMG signals that combine the

$$\varepsilon_i = \sqrt{[(t_{\text{ACT, ALG},i} - t_{\text{ACT,EXP},i})^2 + (t_{\text{DEACT, ALG},i} - t_{\text{DEACT,EXP, }i})^2]}, \quad i = 1, \ldots, 30 \tag{4}$$

TABLE I
MEAN AND STANDARD DEVIATION OF THE PARAMETERS T, w, AND k, OBTAINED WITH THE MINIMIZATION PROCEDURE APPLIED ON 30 STRIDES

PARAMETER	MEAN	STANDARD DEVIATION
T	0.1 [s]	0.04 [s]
w	0.3	0.08
k	0.06	0.03

Gaussian functions and the white noise to realistically approximate the real situations [24]. From this first comparison, two best performing standard algorithms have been extracted (analyzing the differences between the real and measured onsets, and the total number of activations measured). Then these two standard methods have been used in a second comparison against the proposed method, to test its performance with respect to the variation of the parameters of the simulated signal, in particular with respect to the SNR. Finally, the proposed method has been used to measure the muscle timing in real SEMG signals using the acquisition of leg muscles of healthy subjects during gait tasks. The results have finally been compared with the literature values.

A. Comparison With Automatic Methods From the Literature

A list of the 10 common automatic detection methods present in the literature is shown in Table II. Methods from 1 to 5 and method 9 use the baseline level for the onset detection, while methods 6–8 compute the threshold from the maximal contraction. Methods 2 and 5 are suitable only for muscle onset detection, while the other can also measure the muscle offset. Method 10 is more complex because it uses the 95th percentiles of the signal as the threshold for the onset detection.

All different methods were compared using a computer-generated set of artificial SEMG signals that simulate a muscle with a monophasic activation. The signals belong to two classes: 1) signals with a constant resting condition before and after the main activation and 2) signals with residual activations during the resting period before and after the main activation.

The first set of signals is obtained by applying a uniformly distributed stochastic process (white noise) modulated by a single truncated Gaussian function as in (5), as shown at the bottom of this page, where n is the amplitude of the baseline noise, and random is a function that generates a number with values uniformly distributed between zero and one. With n and the RANDOM function, white noise can be generated. The function for the modulation is a Gaussian function centered around t_c. It has an amplitude equal to SNR $* n$, a standard deviation σ, and a width w resulting in a truncation at times $t_c - w/2$ and $t_c + w/2$.

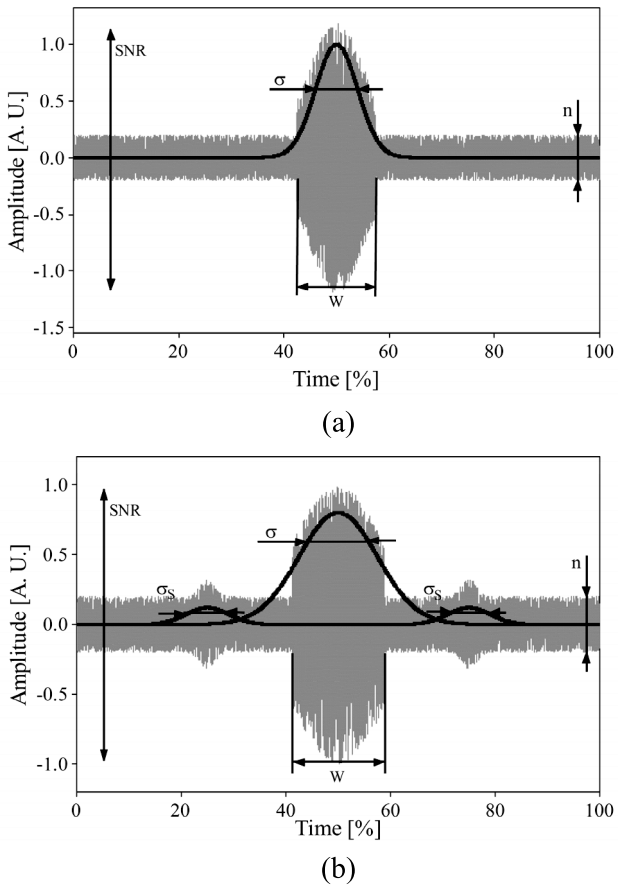

Fig. 2. Example of simulated SEMG signals with (a) constant resting period before and after the main activation and (b) residual bursts during resting period. This figure shows the parameters used for the generation of the signals: SNR is the signal-to-noise ratio, σ is the standard deviation of the Gaussian function used for the modulation of the main activation, n is the noise level, w represents the truncation width of the main Gaussian function, and σ_S is the standard deviation of the Gaussian functions used for the generation of the bursts.

The second set of signals was obtained starting from (5), and modulating the resulting signals with two additional Gaussian functions before and after the main activation using (6), as shown at the bottom of the next page, where the Gaussian functions generating the secondary activations have an amplitude equal to $S * n$, a standard deviation equal to σ_S and are placed to a distance equal to *dist* from the mean time of the main activation.

An example of a simulated SEMG signal from the first class is reported in Fig. 2(a), while a typical signal of the second class is shown in Fig. 2(b).

$$y(t) = \begin{cases} n * \text{RANDOM}(0,1), & \text{when } t < \left(t_C - \dfrac{w}{2}\right) \\ n * \text{RANDOM}(0,1) * \left(1 + \text{SNR} * e^{-\frac{(t-t_C)^2}{2\sigma^2}}\right), & \text{when } \left(t_C - \dfrac{w}{2}\right) \le t \le \left(t_C + \dfrac{w}{2}\right) \\ n * \text{RANDOM}(0,1), & \text{when } t > \left(t_C + \dfrac{w}{2}\right) \end{cases} \quad (5)$$

TABLE II
STANDARD METHODS USED FOR THE FIRST COMPARISON WITH THE PROPOSED ALGORITHM

METHOD	SIGNAL PROCESSING	BASELINE	ONSET DETECTION	REFERENCE
1	Rectification + meaning average (windows width 50ms)	Mean of the firsts 500ms, 2s before the onset	Two consecutive points >2 standard deviation from the baseline activity	[25]
2	Rectification + low-pass filter ($f_{CUT\text{-}OFF}$=40Hz)	Mean of the 100ms before the onset	First deviation>1.5 standard deviation from baseline	[26]
3	Rectification + low-pass filter ($f_{CUT\text{-}OFF}$=50Hz)+meaning average (windows width 20ms)	Mean of the 50ms before the onset	First deviation>3 standard deviation from baseline for at least 25ms	[27]
4	Band-pass filter ($f_{CUT\text{-}OFF,LOW}$=10Hz, $f_{CUT\text{-}OFF,HIGH}$=10Hz) + rectification + meaning average (windows width 40ms)	Mean of the 500ms of quite standing before the onset	First deviation>2 standard deviation from baseline mean and median	[28]
5	Rectification + low-pass filter ($f_{CUT\text{-}OFF}$=100Hz)	Mean of the 100ms of quite standing before the onset	First deviation>2.5 standard deviation from baseline	[29]
6	Band-pass filter ($f_{CUT\text{-}OFF,LOW}$=0.8Hz, $f_{CUT\text{-}OFF,HIGH}$=800Hz) + rectification + meaning average (windows width 100 acquisition points) + subtraction with the mean value	Mean of the 500ms before the onset	First deviation>15% of the maximal contraction	[30]
7	Band-pass filter ($f_{CUT\text{-}OFF,LOW}$=0.8Hz, $f_{CUT\text{-}OFF,HIGH}$=800Hz) + rectification + meaning average (windows width 100 acquisition points) + subtraction with the mean value	Mean of the 500ms before the onset	First deviation>5% of the maximal contraction	[31]
8	Band-pass filter ($f_{CUT\text{-}OFF,LOW}$=0.8Hz, $f_{CUT\text{-}OFF,HIGH}$=800Hz) + rectification + meaning average (windows width 100 acquisition points) + subtraction with the mean value	Mean of the 500ms before the onset	First deviation>25% of the maximal contraction	
9	Rectification + low-pass filter ($f_{CUT\text{-}OFF}$=6Hz)	Mean of the 240ms before the onset	First deviation>1 standard deviation from baseline for at least 8ms (not below for at least 16ms)	[32]
10	Rectification + band-pass filter ($f_{CUT\text{-}OFF,LOW}$=10Hz, $f_{CUT\text{-}OFF,HIGH}$=500Hz)	No baseline	First instant>95 percentile for at least 10ms	[33]

The parameters describing the simulated signals were varied randomly (following a uniform distribution) within the ranges described in Table III. These ranges were set to generate signals that could reasonably approximate the real muscle behavior. Some of the parameters kept a constant value for all the simulations to simplify the evaluation of the proposed algorithm.

The onset time of the simulated signals, to be later considered as the ideal onset for the evaluations that follow, depends on the value of the parameters. We defined it

$$y(t) = \begin{cases} n * \text{RANDOM}(0,1) * \left(1 + S * e^{-\frac{(t-(t_C-\text{dist}))^2}{2\sigma_S^2}}\right), & \text{when } t < \left(t_C - \frac{w}{2}\right) \\ n * \text{RANDOM}(0,1) * \left(1 + \text{SNR} * e^{-\frac{(t-t_C)^2}{2\sigma^2}}\right), & \text{when } \left(t_C - \frac{w}{2}\right) \le t \le \left(t_C + \frac{w}{2}\right) \\ n * \text{RANDOM}(0,1) * \left(1 + S * e^{-\frac{(t-(t_C+\text{dist}))^2}{2\sigma_S^2}}\right), & \text{when } t > \left(t_C + \frac{w}{2}\right) \end{cases} \quad (6)$$

TABLE III
DESCRIPTION AND RANGES OF THE PARAMETERS FOR SEMG SIGNAL SIMULATION

SYMBOL	DESCRIPTION	VALUE
n	Amplitude of the baseline noise	0.2 [mV]
$\mathbf{t_C}$	Mean time of the main Gaussian function	1 [s]
w	Truncation width of the main Gaussian function	0.05÷0.35 [s]
SNR	Signal-to-noise ratio of the main Gaussian function	100÷3 000 [%]
$\boldsymbol{\sigma}$	Standard deviation of the main Gaussian function	0.05÷0.2 [s]
S	Signal-to-noise ratio of the secondary Gaussian function	0.6
dist	Distance of the secondary Gaussian functions from the main one	0.5 [s]
$\boldsymbol{\sigma_S}$	Standard deviation of the secondary Gaussian functions	0.03 [s]

according to

$$t_{\text{ONSET}} = t_C - \frac{w}{2}. \tag{7}$$

For each situation, a set of 10 000 simulated SEMG signals, with known onset, were generated and analyzed. Signals were generated with a sampling frequency of 5 kHz and a signal duration of 2 s. It is worth noting, from the analysis of the generated signals of Fig. 2, that the ideal number of onset times is one in both cases.

B. Number of Activations

The results of the evaluation of the proposed method against the standard methods of Table II are summarized in Fig. 3(a) and (b). Fig. 3(a) and (b) plot the value of the average number μ_N (abscissas) and standard deviation SD_N (ordinates) of the differences between the number of activations detected by each method and the ideal number (we recall that the ideal activation number should be one), for the whole set of 10 000 generated signals. In particular, Fig. 3(a) shows the results of signals with constant resting period, whereas Fig. 3(b) shows the results of signals with residual bursts during the resting period. For each method examined, activations shorter than the minimum duration defined by the method have not been considered.

From Fig. 3(a), we note that all methods, except two, are correctly placed around the origin (low average and low standard deviation). Method 7 exhibits both a large positive average and a large positive standard deviation, whereas method 10 exhibits a negative average, thus indicating a poor ability to detect signal onsets.

From Fig. 3(b), it is evident that the majority of the methods performing well with the simulated signals having a constant resting period, markedly degrade in performance when the resting period has secondary bursts. Both averages and standard deviations thus increase with respect to Fig. 3(a).

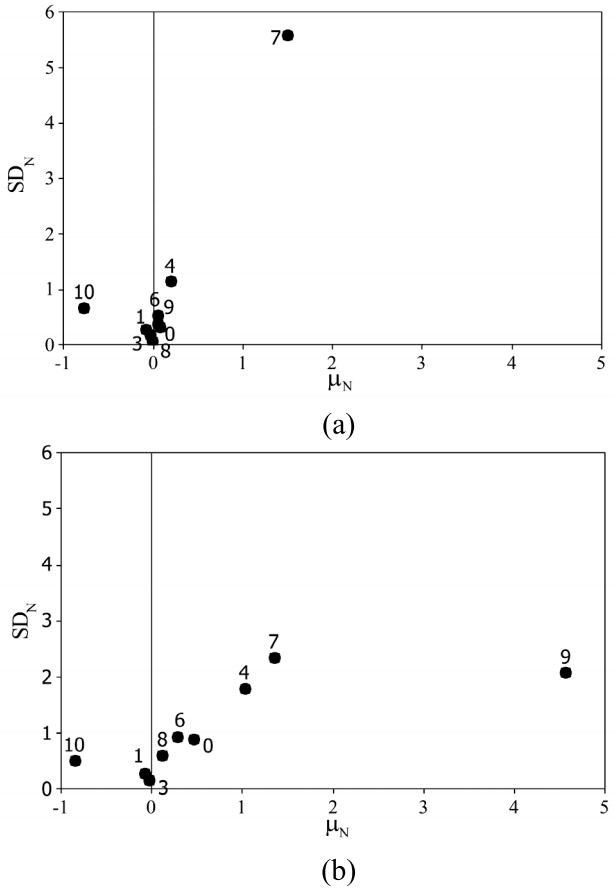

Fig. 3. Mean (μ) and standard deviation (SD) of the differences between the number of activations measured by each method and the real number of activations of the signals, for simulated signals with (a) constant resting period and (b) residual bursts during the resting period. The label number represents each method. Method 0 represents the proposed algorithm.

In Fig. 3(a) and Fig. 3(b), methods 2 and 5 are not plotted being out of the graphs area. This is due to the fact that these methods are optimized only for onset detection and not for offset detection, and this results in an excessive number of false activations. Of all the other methods, our method 0 is located among the best five, as it is evident both in Fig. 3(a) and (b).

Other than our method, the best performer for signals of Fig. 3(a) is method 8 ($\mu_N = 2 \times 10^{-3}$, $\text{SD}_N = 0.06$), immediately followed by method 3 ($\mu_N = 26 \times 10^{-3}$, $\text{SD}_N = 0.17$), whereas for signals with residual bursts, the best performer is method 3 ($\mu_N = 23 \times 10^{-3}$, $\text{SD}_N = 0.16$). Thus, method 3 is chosen as one of the benchmarks for the second comparison.

C. Activation Timing

Differences between the measured and the real onset time are an adequate indicator of the accuracy of a detection method. Low values of average and standard deviation indicate a high accuracy in the determination of the muscular timing. Positive mean values indicate a delayed onset compared with the ideal case.

Fig. 4(a) and (b) shows the average μ_t and the standard deviation SD_t of the difference between the onset time measured by each method and the ideal onset time [from (6)] of

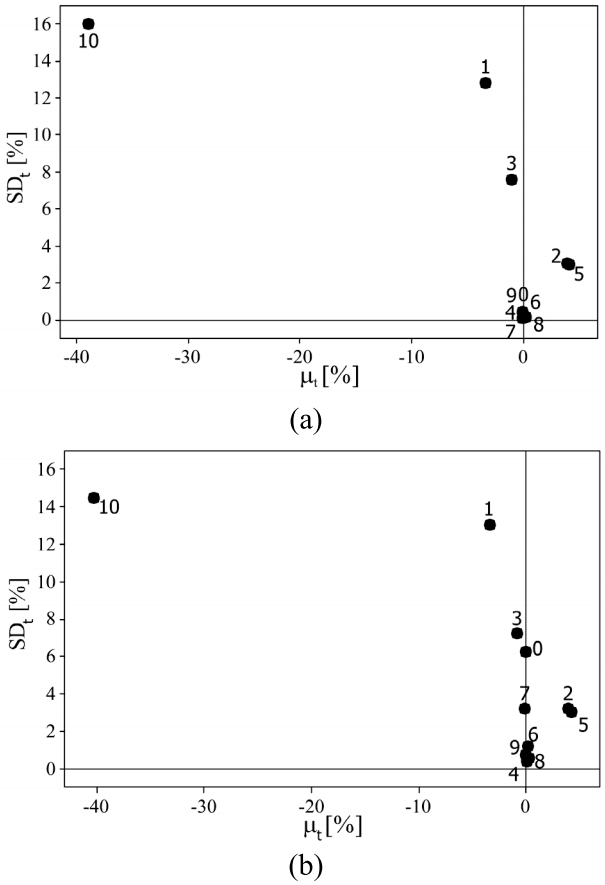

Fig. 4. Mean (μ) and standard deviation (SD) of the differences between the onsets measured by each method and the real onsets of the signals, with respect to the signals duration, for simulated signals with (a) constant resting period and (b) residual bursts during the resting period. The label number represents each method. Method 0 represents the proposed algorithm.

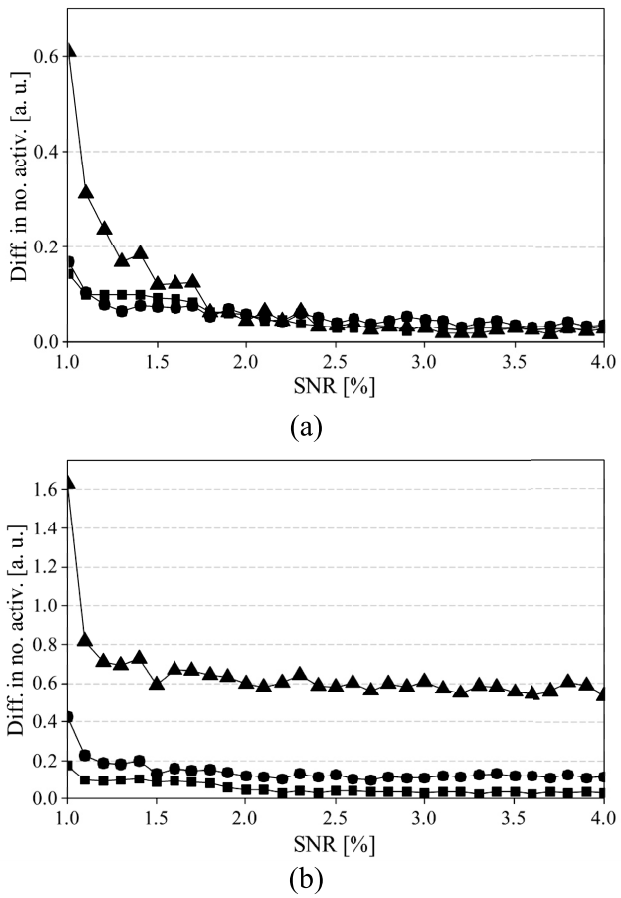

Fig. 5. RMS values of the differences between the measured and the ideal number of activations with respect to the SNR of the simulated signals for the proposed method (•), for method 3 (■), and for method 9 (▲), for simulated signals with (a) constant resting period and (b) residual bursts during the resting period.

the simulated signals, respectively, for signals with constant resting period and with residual bursts during the resting period. The differences are computed with respect to the simulated signals duration. If more than one activation is measured, only the longer one is considered for the mean and standard deviation computation.

Again, all methods perform better in the case of signals with constant resting period [Fig. 4(a)] than in the case of signals with residual bursts [Fig. 4(b)]. However, this difference is less marked, suggesting that the parameter μ_t is less sensitive to residual bursts than parameter μ_n. Our method 0 shows a good behavior in both situations despite a somewhat larger value of SD_t in the case of residual bursts ($\mu_t = 18.5 \times 10^{-3}$ s and $SD_t = 0.46$ s in Fig. 4(a) and $\mu_t = 69.2 \times 10^{-3}$ s and $SD_t = 6.27$ s in Fig. 4(b). This increase is probably related to the occasional presence of residual bursts very close to the main activation: in this case our method considers the bursts as a part of the main activation.

For both situations, the best performers are method 9 ($\mu_t = -1.5 \times 10^{-3}$ s and $SD_t = 0.41$ s for signals with constant resting period and $\mu_t = -10.9 \times 10^{-3}$ s and $SD_t = 0.74$ s for signals with residual bursts), followed by method 4 ($\mu_t = -11.4 \times 10^{-3}$ s and $SD_t = 0.12$ s for signals with constant resting period and $\mu_t = 62.7 \times 10^{-3}$ s and $SD_t = 0.36$ s for signals with residual bursts).

In conclusion, method 9 is chosen as the best performer and will be used for the next comparison.

D. Comparison With the Best Performers

Following the choice of the two best performers 3 and 9 to be compared with our method, we investigated the dependence of all three methods on the SNR of the electromyographic signal. The choice of SNR as the independent variable is motivated by the fact that this parameter is exclusively related to the acquisition instrumentation, and can be easily quantified (other parameters, such as σ and w, are muscle dependent and less controllable). Fig. 5 shows the rms values of the difference between the number of activations measured by each method and the ideal number of activations (1) of the simulated signals, as a function of the signal SNR of the simulated signals. The rms value is here considered to keep into account both stochastic and systematic effects in one single value. Of the two graphs, again the former refers to signals with constant resting period, the latter to signals with residual bursts during the resting period.

As expected, all methods show a monotonic decrease with increasing SNR. From Fig. 5(a) and (b), we note that our method 0, and method 3 perform significantly better than method 9 for all SNR values, the two methods performing

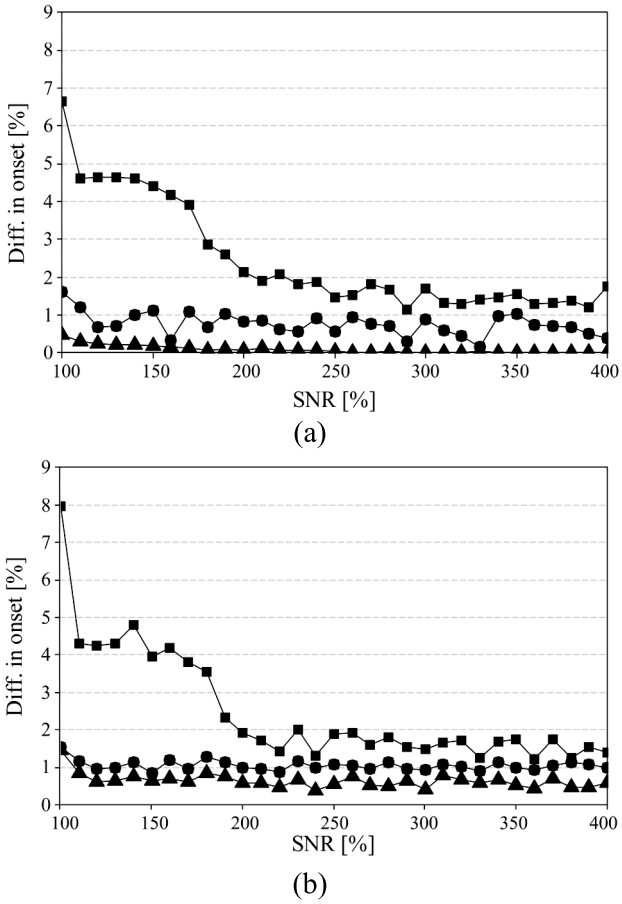

Fig. 6. RMS values of the differences between the measured and real onsets with respect to the SNR of the simulated signals for the proposed method (●), for method 3 (■), and method 9 (▲), for simulated signals with (a) constant resting period and (b) residual bursts during the resting period.

equally well with signals without residual bursts, and method 3 performing slightly better than ours with signals with residual bursts.

Fig. 6(a) (signals without bursts) and (b) (signals with bursts) shows the dependence of the difference in onset timing (expressed as a percentage of the simulated signal duration), again as a function of SNR, as a mean to understand how noise affects the ability of the method to correctly locate the muscle onset time. We clearly observe that, in this case, the situation is opposite with respect to the case of Fig. 5. Here, in fact, our method 0 and method 9 are the best performers at all SNR values and for both types of signals, whereas method 3 performs significantly worse. This is evident in particular in the case of signals with residual bursts.

As a result of both sets of figures, we can conclude that our method is the best performing method as far as the number of activations and activation timing is concerned.

E. Tests in Clinical Environment

Finally, our method has been tested in the clinical context to measure the onsets and offsets of real SEMG signals acquired from leg muscles of 10 healthy subjects during gait tasks (only healthy subjects were chosen to simplify the comparison

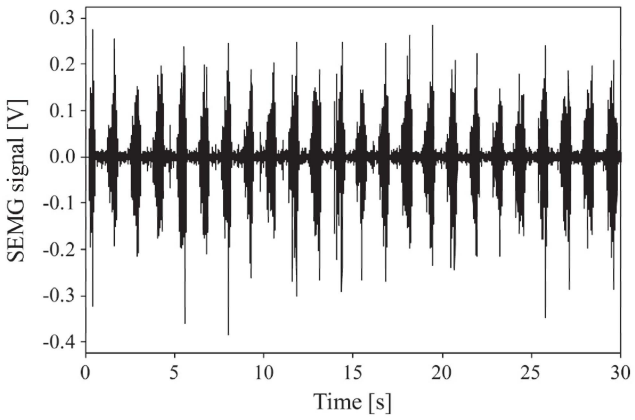

Fig. 7. Example of SEMG signal acquired from a subject performing gait task on a treadmill at a walking speed of 3.2 km/h.

with the literature data). For each subject, signals from the *tibialis anterior* muscle, the *soleus* muscle, and the *hamstring* muscle of each leg were acquired using surface electrodes coupled to the skin by means of a conductive gel. Electrodes were placed on the skin using the guidelines in [34].

The subjects were asked to perform gait tasks on different surfaces (floor and treadmill) and at different walking speeds (1.8, 2.5, and 3.2 km/h). As a result, 900 steps were recorded and analyzed from the subjects. Pressure sensors were placed under the subjects' feet to sense heel contacts. If more than one onset (or offset) is measured, only the longer one is considered for the computation of mean and standard deviation. Fig. 7 shows an example of a signal acquired from a subject during a walking task on a treadmill at a walking speed of 3.2 km/h. SEMG signals were acquired using an electromyographer BTS FreeEMG 300 (rate 1 kHz). SEMG signals were acquired for 30 s during the walking task. Signals were divided using foot-switch sensors placed under the left and right toes and the left and right heels to recognize each step. Acquired signal did not need to be filtered apart from hardware filtration performed by electromyographer.

The results of these tests are summarized in Fig. 8 (for the sake of simplicity, only data from the *soleus* muscle are reported). Mean (dots) and standard deviation (bars) of the onset [Fig. 8(a)] and of the offset [Fig. 8(b)] timing (again as a percentage of the cycle duration) are shown for all 10 subjects, differentiated for each subject between left and right legs. Fig. 8 shows that there is a maximum standard deviation equal to 8.3% for the onset and 4.2% for the offset (intrasubject repeatability), both for the subject no. 5, right side. From Fig. 8, we note that all the onsets [Fig. 8(a)] are located within a band of 21% (intersubject repeatability) around the average value of 24.2%, whereas the offsets [Fig. 8(b)] are located within a band of 11.9% (intersubject repeatability) around the average value of 59.2%.

The intrasubject and intersubject repeatability is therefore quite satisfactory, and compatible with the normal variability of subjects performing gait task at different speeds. The results obtained are well consistent with the well-agreed literature data, which place muscle onsets between 15% and 25% of

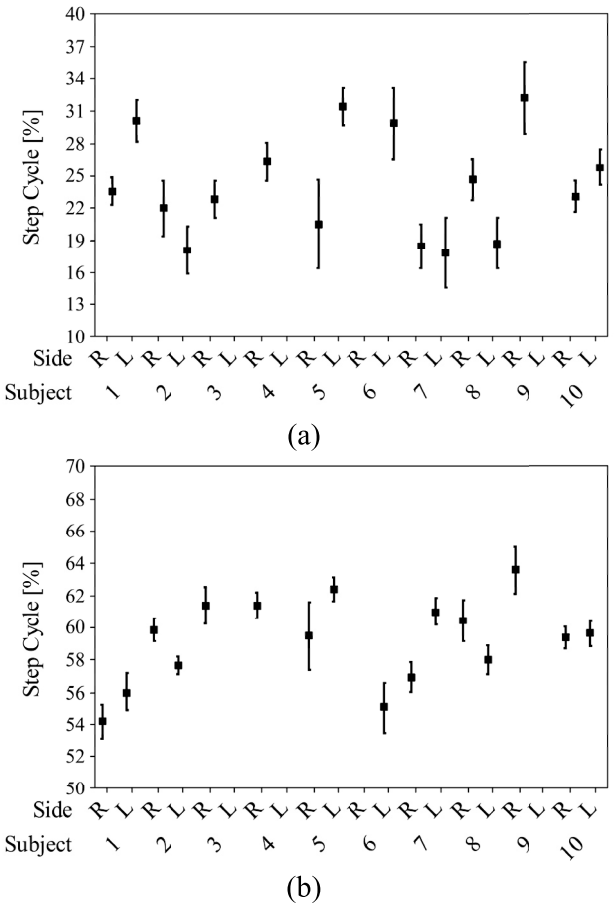

Fig. 8. (a) Onset and (b) offset of the *soleus* muscle measured by the proposed algorithm in real SEMG signals, acquired from healthy subjects, during gait tasks. The results show the mean (square) and the standard deviation (bars) of the onset and the offset measured on the whole number of steps of each subject for the left side (L) and for the right side (R).

the step cycle, and offsets between 50% and 60% of the step cycle [23].

Analysis on the *tibialis anterior* muscle and the *hamstring* muscle give similar results, with the main activation compatible with the well-agreed literature data.

IV. Conclusion

A new algorithm for muscle timing detection has been proposed and verified using both simulated and real SEMG signals. It uses a statistical approach for threshold computation and avoids the necessity of a maximum voluntary contraction, or baseline level measurements. The results show that, for each parameter analyzed, the proposed algorithm is comparable with the best performing method, which is different if the number of activations detected or the activation timing were considered. The verification on real SEMG signals confirms the good behavior of the proposed algorithm, showing the results comparable with the literature data.

This suggests that the proposed algorithm is more suitable for applications where the measurement of the total number of muscle activations and a good accuracy in onset detection are required and when is not possible to measure the maximal voluntary contraction or the baseline level.

References

[1] C. Frigo and P. Crenna, "Multichannel SEMG in clinical gait analysis: A review and state-of-the-art," *Clin. Biomech.*, vol. 24, no. 3, pp. 236–245, Mar. 2009.

[2] F. Hug, "Can muscle coordination be precisely studied by surface electromyography?" *J. Electromyogr. Kinesiol.*, vol. 21, no. 1, pp. 1–12, Feb. 2011.

[3] Y. Su, M. H. Fisher, A. Wolczowski, G. D. Bell, D. J. Burn, and R. X. Gao, "Towards an EMG-controlled prosthetic hand using a 3-D electromagnetic positioning system," *IEEE Trans. Instrum. Meas.*, vol. 56, no. 1, pp. 178–186, Feb. 2007.

[4] B. Biljan, Z. Potocanac, and M. Cifrek, "Comparison of two muscle activity detection techniques from surface EMG signals applied to countermovement jump," in *Proc. IFMBE*, vol. 37. 2012, pp. 834–837.

[5] P. W. Hodges and B. H. Bui, "A comparison of computer-based methods for the determination of onset of muscle contraction using electromyography," *Electroencephalogr. Clin. Neurophysiol./Electromyogr. Motor Control*, vol. 101, no. 6, pp. 511–519, Dec. 1996.

[6] S. Lewis *et al.*, "Fully implantable multi-channel measurement system for acquisition of muscle activity," *IEEE Trans. Instrum. Meas.*, vol. 62, no. 7, pp. 1972–1980, Jul. 2013.

[7] H. I. Dubo *et al.*, "Electromyographic temporal analysis of gait: Normal human locomotion," *Arch. Phys. Med. Rehabil.*, vol. 57, no. 9, pp. 415–420, Sep. 1976.

[8] A. B. Arsenault, D. A. Winter, R. G. Marteniuk, and K. C. Hayes, "How many strides are required for the analysis of electromyographic data in gait?" *Scandin. J. Rehabil. Med.*, vol. 18, no. 3, pp. 133–135, Feb. 1986.

[9] E. Fiorucci, G. Bucci, R. Cattaneo, and A. Monaco, "The measurement of surface electromyographic signal in rest position for the correct prescription of eyeglasses," *IEEE Trans. Instrum. Meas.*, vol. 61, no. 2, pp. 419–428, Feb. 2012.

[10] A. Merlo, D. Farina, and R. Merletti, "A fast and reliable technique for muscle activity detection from surface EMG signals," *IEEE Trans. Biomed. Eng.*, vol. 50, no. 3, pp. 316–323, Mar. 2003.

[11] L. Li and G. E. Caldwell, "Muscle coordination in cycling: Effect of surface incline and posture," *J. Appl. Physiol.*, vol. 85, no. 3, pp. 927–934, Sep. 1998.

[12] S. Dorel, A. Couturier, and F. Hug, "Intra-session repeatability of lower limb muscles activation pattern during pedaling," *J. Electromyogr. Kinesiol.*, vol. 18, no. 5, pp. 857–865, Oct. 2008.

[13] G. J. W. Mallory and R. Doraiswami, "A filter for on-line estimation of spectral content," *IEEE Trans. Instrum. Meas.*, vol. 48, no. 6, pp. 1047–1055, Dec. 1999.

[14] G. D. Fraser, A. D. C. Chan, J. R. Green, and D. T. Macisaac, "Automated biosignal quality analysis for electromyography using a one-class support vector machine," *IEEE Trans. Instrum. Meas.*, vol. 63, no. 12, pp. 2919–2930, Dec. 2014.

[15] A. M. Burden, S. E. Lewis, and E. Willcox, "The effect of manipulating root mean square window length and overlap on reliability, inter-individual variability, statistical significance and clinical relevance of electromyograms," *Manual Therapy*, vol. 19, no. 6, pp. 595–601, 2014.

[16] A. Avila and J.-Y. Chang, "EMG onset detection and upper limb movements identification algorithm," *Microsyst. Technol.*, vol. 20, nos. 8–9, pp. 1635–1640, Aug. 2014.

[17] G. Kamen and D. A. Gabriel, "EMG signal processing," in *Essentials of Electromyography*, 1st ed. Champaign, IL, USA: Human Kinetics Pub., 2010, pp. 112–114.

[18] M. Mulas, M. Folgheraiter, and G. Gini, "An EMG-controlled exoskeleton for hand rehabilitation," in *Proc. 9th ICORR*, Chicago, IL, USA, Jun./Jul. 2005, pp. 371–374.

[19] R. Song, K.-Y. Tong, X. Hu, and L. Li, "Assistive control system using continuous myoelectric signal in robot-aided arm training for patients after stroke," *IEEE Trans. Neural Syst. Rehabil. Eng.*, vol. 16, no. 4, pp. 371–379, Aug. 2008.

[20] T. D. Lalitharatne, Y. Hayashi, K. Teramoto, and K. Kiguchi, "A study on effects of muscle fatigue on EMG-based control for human upper-limb power-assist," in *Proc. 6th ICIAfS*, Beijing, China, Sep. 2012, pp. 124–128.

[21] I. Elamvazuthi, K. A. E. K. Nurhanim, P. Vasant, S. Parasuraman, Z. Zulika, and G. A. Ling, "Surface electromyogram (sEMG) detection and analysis in the development of an exoskeleton control system," in *Proc. 2nd AUCC*, Sydney, NSW, Australia, Nov. 2012, pp. 197–202.

[22] BIPM, IEC, IFCC, ILAC, ISO, IUPAC, IUPAP, and OIML, *International Vocabulary of Metrology—Basic and General Concepts and Associated Terms (VIM)*, 3rd ed., document JCGM, 2008.

[23] D. A. Newmann, "Kinesiology of walking," in *Kinesiology of the Musculoskeletal System*. Amsterdam, The Netherlands: Elsevier, 2003, pp. 547–551.
[24] P. Bonato, T. D'Alessio, and M. Knaflitz, "A statistical method for the measurement of muscle activation intervals from surface myoelectric signal during gait," *IEEE Trans. Biomed. Eng.*, vol. 45, no. 3, pp. 287–299, Mar. 1998.
[25] E. J. Neafsey, C. D. Hull, and N. A. Buchwald, "Preparation for movement in the cat. II. Unit activity in the basal ganglia and thalamus," *Electroencephalogr. Clin. Neurophysiol.*, vol. 44, no. 6, pp. 714–723, Jun. 1978.
[26] L. M. Nashner, A. Shumway-Cook, and O. Marin, "Stance posture control in select groups of children with cerebral palsy: Deficits in sensory organization and muscular coordination," *Experim. Brain Res.*, vol. 49, no. 3, pp. 393–409, Mar. 1983.
[27] R. P. Di Fabio, "Reliability of computerized surface electromyography for determining the onset of muscle activity," *Phys. Therapy*, vol. 67, no. 1, pp. 43–48, Jan. 1987.
[28] W. A. Lee, T. S. Buchanan, and M. W. Rogers, "Effects of arm acceleration and behavioral conditions on the organization of postural adjustments during arm flexion," *Exp. Brain Res.*, vol. 66, no. 2, pp. 257–270, 1987.
[29] C. M. Chanaud and J. M. Macpherson, "Functionally complex muscles of the cat hindlimb. III. Differential activation within biceps femoris during postural perturbations," *Exp. Brain Res.*, vol. 85, no. 2, pp. 271–280, 1991.
[30] J. E. Bullock-Saxton, V. Janda, and M. I. Bullock, "Reflex activation of gluteal muscles in walking. An approach to restoration of muscle function for patients with low-back pain," *Spine*, vol. 18, no. 6, pp. 704–708, May 1993.
[31] J. E. Bullock-Saxton, "Local sensation changes and altered hip muscle function following severe ankle sprain," *Phys. Therapy*, vol. 74, no. 1, pp. 17–28, Jan. 1994.
[32] C. Steele, "Anticipatory postural reactions in clumsy children: Changes after physiotherapy treatment," M.S. thesis, Dept. Health Behavioral Sci., Univ. Queensland, Brisbane, QLD, Australia, 1994.
[33] H. W. Thompson and P. A. McKinley, "Landing from a jump: The role of vision when landing from known and unknown heights," *Neuroreport*, vol. 6, no. 3, pp. 581–584, Feb. 1995.
[34] A. O. Perotto, "Leg," in *Anatomical Guide for the Electromyographer*, 3rd ed. Springfield, IL, USA: Charles C. Thomas, 1994, pp. 142–173.

Simone Pasinetti received the B.S. and M.S. (Hons.) degrees in automation engineering from the University of Brescia, Brescia, Italy, in 2009 and 2011, respectively, with a thesis concerning the control of mechanical actuators with surface electromyography signals, and the Ph.D. degree in applied mechanics from the University of Brescia, in 2015. His Ph.D. thesis was entitled Development of Measurement Protocols for the Analysis of the Functional Evaluation and Rehabilitation in Biomechanics Field.

He was with the Institute of Intelligent Systems and Robotics, Paris, France, during the Ph.D., where he was involved in research on the dynamic posture analysis. Since 2015, he has been a Research Fellow with the Optoelectronics Laboratory, University of Brescia. He is currently involved in posture analysis and liquid lenses system development. His current research interests include biomechanics of human posture, EMG analysis, and 2-D and 3-D vision system development.

Matteo Lancini received the master's degree in mechanical engineering and the Ph.D. degree in applied mechanics from the University of Brescia, Brescia, Italy, in 2005 and 2015, respectively.

He was a Research Contractor with the Department of Industrial and Mechanical Engineering, University of Brescia, where he was involved in the development of measurement techniques for industrial diagnostics, and focused on measurements in uncontrolled environments from 2005 to 2009. He is currently an Assistant Professor with the Mechanical and Thermal Measurements Laboratory, Department of Industrial and Mechanical Engineering, University of Brescia. His current research interests include measurement systems for biomechanical analysis, in particular, for robotic gait and rehabilitation, and industrial diagnostics using nondestructive techniques based on vibration measurements.

Mr. Lancini is a member of the International Society of Biomechanics.

Ileana Bodini received the master's degree in mechanical engineering from the University of Brescia, Brescia, Italy, in 2006, with a thesis concerning the design of innovative measurement systems based on cosmic ray detection. She received the Ph.D. degree from the University of Padua, Padua, Italy, in 2010, with a thesis concerning the development of diagnostic non-destructive techniques, based on vibrational measurements, for industrial applications.

She has worked with the group of Fundamental and Applied Nuclear Physics, University of Brescia, in 2006, performing Monte–Carlo simulations and analysing the resulting data for the EURITRAK Project (FP6, priority 2, IST, contract n° 511 471). From 2007 to 2014, she was with the Group of Mechanical and Thermal Measurement, University of Brescia, and she was involved in the development of measurement systems for industrial applications and in the development of diagnostic nondestructive techniques for industrial, aerospace and civil applications. Since 2014, she has been with the Laboratory of Optoelectronics, University of Brescia (Department of Information Engineering) as a Research Fellow. Her current research interests include design and dimensioning of 2-D and 3-D vision (embedded and nonembedded) systems for research and industrial application; the development of measurement devices based on vision systems, and techniques for industrial measurements and diagnostic based on vision systems and image processing.

Franco Docchio received the M.S. degree from the Polytechnic of Milan, Milan, Italy, in 1976.

He was with the Centro di Elettronica Quantistica of Italy from 1978 to 1987, where he was involved in research on laser development, laser applications in industry and bio-medicine and laser-tissue interaction. In 1987, he joined the Dipartimento di Elettronica per l'Automazione, University of Brescia, Brescia, Italy, where he currently holds the Full Professorship in electrical measurements. He is a member of the Laboratory of Optoelectronics with the University of Brescia. In the Laboratory, he has been involved in projects of basic and applied research, in collaboration with international institutions and companies. In recent years, within the activities of the Laboratory, he has been active in the creation and incubation of a number of Spin-Off companies, that operate in the domain of Optoelectronics, laser processing of materials, optical sensors, and 3-D vision. He has authored over 220 publications, mostly international. He has deposited five international patents on instrumentation and innovative techniques for electrooptical measurements.

Mr. Docchio is a fellow of the European Optical Society.